Auger and Coster-Kronig Transition Probabilities to the Atomic 2s State and Theoretical L_1 Fluorescence Yields*

Bernd Crasemann and Mau Hsiung Chen
Department of Physics, University of Oregon, Eugene, Oregon 97403

and

Vaclav O. Kostroun
Ward Reactor Laboratory, Department of Applied Physics, Cornell University, Ithaca, New York 14850

(Received 30 June 1971)

Atomic L_1-level Auger and Coster-Kronig widths have been calculated for 14 elements with $33 \leq Z \leq 85$. Nonrelativistic screened hydrogenic wave functions and j-j coupling were used; all pertinent transitions were included that involve final vacancy configurations through $f_{7/2}f_{7/2}$. With the aid of Scofield's x-ray emission rates, L_1 fluorescence yields are calculated. Total L_1, L_2, and L_3 level widths are compared.

I. INTRODUCTION

In two previous papers,[1,2] we have reported on the calculation of radiationless transition probabilities to the atomic K, L_2, and L_3 shells. The results were combined with the x-ray emission rates computed by Scofield[3] to find fluorescence yields. We now complete this work by reporting analogous results for the L_1 shell. The difficulty of ascertaining realistic inner-shell electron binding energies in ionized atoms, which had caused us to postpone the L_1-shell work, has been overcome only in part through use of the electron-spectroscopy-for-chemical-analysis (ESCA) tables[4] of neutral-atom ionization thresholds and consideration of available experiment data; some uncertainty remains regarding the atomic numbers at which discontinuities in the 2s Auger width occur.

II. THEORY

Radiationless transition probabilities were calculated from nonrelativistic screened hydrogenic single-particle wave functions in j-j coupling.

Bound-state wave function were screened according to Hartree[5]: The effective nuclear charge was chosen so that the mean hydrogenic radial distance of the electron is equal to the mean distance computed from the neutral-atom Hartree-Fock wave functions of Froese.[6] For the continuum wave function, the effective charge was taken to be the geometric mean of the effective charge for the state from which the continuum electron originates and the charge pertaining to the next higher state.[1,2]

Spherical symmetry of the potential was assumed, and the electrostatic interaction potential was ex-

TABLE I. L_1-subshell Auger widths $\Gamma_A(L_1)$, total widths $\Gamma(L_1)$, fluorescence yields ω_1, L_1-L_2X Coster-Kronig widths $\Gamma_A(L_1L_2)$, L_1-L_3X Coster-Kronig widths $\Gamma_A(L_1L_3)$, and radiationless Coster-Kronig transition probabilities a_{12} and a_{13}, as calculated in the present work. All widths are given in eV.

Element	$\Gamma_A(L_1)$	$\Gamma(L_1)$	ω_1	$\Gamma_A(L_1L_2)$	$\Gamma_A(L_1L_3)$	a_{12}	a_{13}
$_{33}$As	1.180	6.962	0.00140	1.961	3.811	0.282	0.547
$_{36}$Kr	1.447	7.688	0.00219	1.726	4.498	0.225	0.585
$_{40}$Zr	1.614	7.930	0.00396	2.148	4.137	0.271	0.522
$_{42}$Mo	1.649	6.497	0.00634	0.311	4.496	0.0479	0.692
$_{47}$Ag	1.747	7.555	0.0101	0.483	5.249	0.0639	0.695
$_{50}$Sn	1.835	8.253	0.0130	0.595	5.716	0.0721	0.693
$_{51}$Sb	1.873	3.825	0.0311	0.626	1.207	0.164	0.316
$_{56}$Ba	2.016	4.464	0.0446	0.750	1.499	0.168	0.336
$_{60}$Nd	2.089	4.719	0.0600	0.778	1.569	0.165	0.332
$_{67}$Ho	2.159	5.247	0.0936	0.934	1.663	0.178	0.317
$_{70}$Yb	2.130	5.430	0.112	0.977	1.714	0.180	0.316
$_{74}$W	2.196	5.812	0.138	0.930	1.881	0.160	0.324
$_{80}$Hg	2.216	12.106	0.0983	1.220	7.480	0.101	0.618
$_{85}$At	2.224	12.570	0.129	1.034	7.690	0.0823	0.612

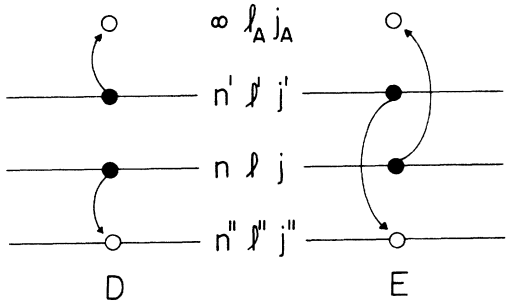

FIG. 1. Schematic representation of direct (D) and exchange (E) Auger transitions, illustrating the designation of pertinent quantum numbers.

panded in terms of scalar products of irreducible tensor operators,[1] so that the Auger matrix elements could be separated into radial and angular factors:

$$1/r_{12}=\sum_{\nu,\sigma}\gamma_\nu(r_1,r_2)C^*_{\nu\sigma}(\Omega_1)\,C_{\nu\sigma}(\Omega_2)\,, \tag{1}$$

where

$$\gamma_\nu(r_1,r_2)=\begin{cases} r_1^\nu/r_2^{\nu+1}, & r_1<r_2 \\ r_2^\nu/r_1^{\nu+1}, & r_2<r_1 \end{cases}, \tag{2}$$

$$C_{\nu\sigma}=[4\pi/(2\nu+1)]^{1/2}\,Y_{\nu\sigma}(\Omega)\,, \tag{3}$$

the $Y_{\nu\sigma}$ being spherical harmonics.

The angular factors in the Auger matrix elements

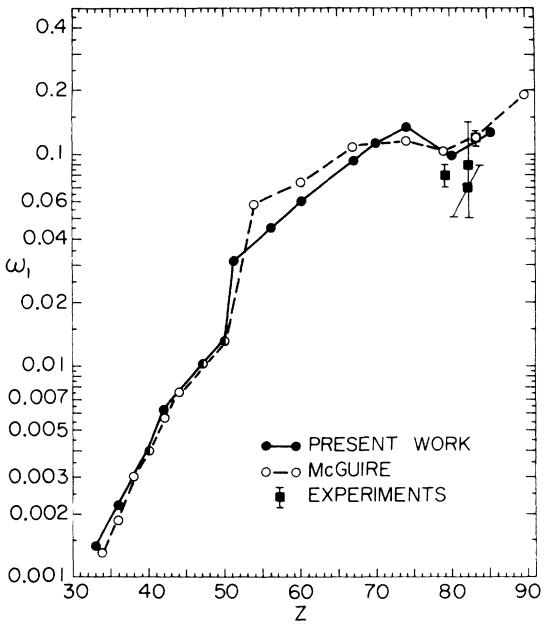

FIG. 2. Theoretical L_1-subshell fluorescence yields ω_1 from the present work and after McGuire (Ref. 10), as functions of atomic number. Experimental results are identified in Table II.

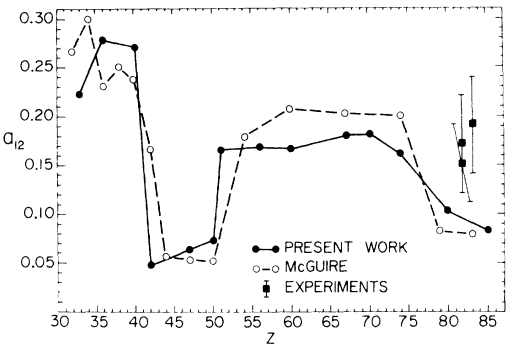

FIG. 3. Radiationless L_1-L_2X Coster-Kronig transition probabilities a_{12} calculated in the present work and by McGuire (Ref. 10), as functions of atomic number. Experimental points represent measured values of f_{12} (Table II).

were computed in j-j coupling. All transitions were included that involve electrons through the $4f_{7/2}$ level. Tables listing the entire set of radiationless transition probabilities in terms of radial matrix elements $\{(nl)(n'l'),\ \nu, l_A\}$ are available from the authors on request.[7,8] In this notation, basically introduced by Asaad and Burhop,[9] the quantum numbers nl characterize the electron that fills the primary vacancy in the direct process, while the electron described by $n'l'$ is ejected into a continuum state with orbital angular momentum $l_A\hbar$. In the exchange process, the $n'l'$ electron fills the original vacancy and the nl electron is ejected (Fig. 1). The index ν pertains to the expansion (1) of $1/r_{12}$; thus, the direct radial matrix elements are of the form

$$\{(nl)(n'l'),\ \nu,\ l_A\}=e^2\int_{r_1,r_2=0}^{\infty}\gamma_\nu R_{n''l''}(r_1)R_{nl}(r_1) \times R_{n'l'}(r_2)R^{l_A}_{\infty}(r_2)r_1^2r_2^2\,dr_1dr_2\,, \tag{4}$$

where the R's are radial wave functions. A complete analytic expression for the radial matrix elements is derived in Ref. 1.

TABLE II. Measured L_1-subshell fluorescence yields ω_1, L_1-L_2X Coster-Kronig probabilities f_{12}, and L_1-L_3X Coster-Kronig probabilities f_{13}.

Element	ω_1	f_{12}	f_{13}	Ref.
$_{77}$Ir			0.46±0.06	11
$_{78}$Pt			0.50±0.05	11
$_{79}$Au	0.08±0.01			12
$_{79}$Au			0.61±0.07	11
$_{81}$Tl			0.57±0.10	13
$_{82}$Pb	0.07±0.02	0.15±0.04	0.57±0.03	14
$_{82}$Pb	0.09±0.02	0.17±0.05	0.61±0.08	15
$_{83}$Bi	0.12±0.01	0.19±0.05	0.58±0.05	16
$_{83}$Bi	0.095±0.005	0.18±0.02	0.58±0.02	17

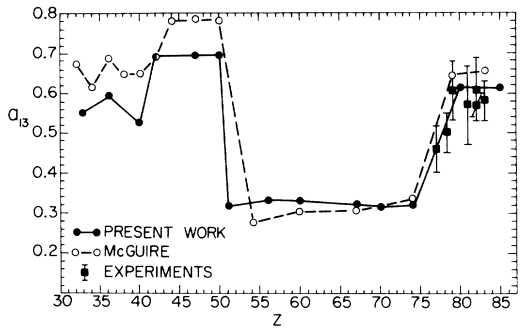

FIG. 4. Radiationless L_1-L_3X Coster-Kronig transition probabilities a_{13} from the present work and according to McGuire (Ref. 10), as functions of atomic number. Experimental points indicate measured values of f_{13}; these are identified in Table II.

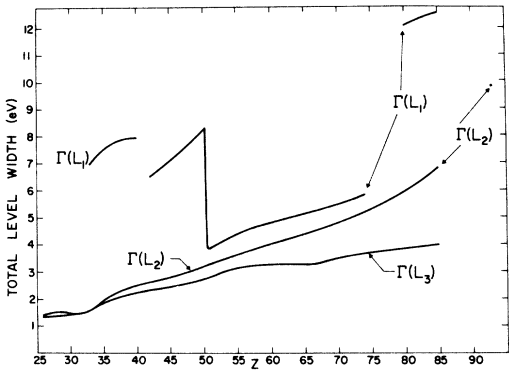

FIG. 5. Total L_1, L_2, and L_3 level widths, as functions of atomic number, according to the present work and Ref. 2.

III. RESULTS AND DISCUSSION

L_1-level radiationless widths $\Gamma_A(L_1)$, computed in the present work, are listed in Table I. Total level widths $\Gamma(L_1)$ are also listed; these were found by adding Scofield's radiative widths[3] $\Gamma_R(L_1)$ to Γ_A. The L_1 fluorescence yield ω_1 is then easily found:

$$\omega_1 = \Gamma_R(L_1)/\Gamma(L_1). \tag{5}$$

The fluorescence yields ω_1 are plotted in Fig. 2 as a function of atomic number. For comparison, the recent results of McGuire[10] are also shown, which were calculated on the basis of exact solutions of the Schrödinger equation in an approximate Herman-Skillman (Hartree-Slater) potential. McGuire used LS coupling for Auger rates and j-j coupling for Coster-Kronig rates; however, the total transition rates are independent of the coupling because the wave functions in the various schemes are related by unitary transformations.[1] The differences between McGuire's and our results, therefore, are due to differences in the radial wave functions. Results of the two sets of calculations are in quite satisfactory agreement. There also is reasonable agreement with the few available measurements[11–17] (Table II); the need for more experimental work is obvious.

Partial widths that correspond to the radiationless L_1-L_2X and L_1-L_3X Coster-Kronig rates have also been computed and are included in Table II. The respective radiationless Coster-Kronig probabilities a_{12} and a_{13} are listed as well. These latter probabilities are plotted in Figs. 3 and 4, respectively, and are compared with McGuire's theoretical results[10] and with measured Coster-Kronig probabilities f_{12} and f_{13} (Table II). It should be noted that the Coster-Kronig probabilities contain a radiative part ω_{ij}:

$$f_{12} = a_{12} + \omega_{12},\ f_{13} = a_{13} + \omega_{13}. \tag{6}$$

The L_1-L_3 radiative rates have been calculated by Scofield[3]; they are small (e.g., $\omega_{13} = 0.0003a_{13}$ for Kr and $\omega_{13} = 0.05a_{13}$ for Hg). The L_1-L_2 radiative transitions, involving a smaller energy difference, are expected to be even less probable.

Total L_1-level widths are shown in Fig. 5 as a function of Z; previously calculated[2] L_2 and L_3 widths are included for comparison. Sharp discontinuities in $\Gamma(L_1)$ occur at the energy thresholds for certain intense groups of Auger transitions, notably near $Z = 41$, 50, and 75. Because the electron binding energies in atoms with inner vacancies are subject to considerable uncertainties, the exact atomic numbers at which the L_1-width discontinuities occur are in doubt. Auger-electron spectroscopy and experimental measurements of level widths could clarify the issue.

ACKNOWLEDGMENTS

It is a pleasure to acknowledge correspondence with Dr. E. J. McGuire of the Sandia Laboratories and discussions with Professor P. Venugopala Rao of Emory University.

*Work supported in part by the U. S. Atomic Energy Commission.

[1] V. O. Kostroun, M. H. Chen, and B. Crasemann, Phys. Rev. A 3, 533 (1971).

[2] M. H. Chen, B. Crasemann, and V. O. Kostroun, Phys. Rev. A 4, 1 (1971).

[3] J. H. Scofield, Phys. Rev. 179, 9 (1969).

[4] K. Siegbahn *et al.*, *ESCA, Atomic, Molecular and Solid State Studies by Means of Electron Spectroscopy* (Nova Acta Regiae Societatis Upsaliensis, Uppsala, 1967), Ser. IV, Vol. 20.

[5] D. Hartree, *The Calculation of Atomic Structures* (Wiley, New York, 1957), Chap. 7.

[6] C. Froese, University of British Columbia report,

1966 (unpublished).

[7]B. Crasemann, M. H. Chen, and V. O. Kostroun, University of Oregon Nuclear Physics Report No. RLO-1925-53, 1971 (unpublished).

[8]Tables for transitions that involve final f holes have also been compiled by E. J. McGuire, Sandia Laboratories Research Report No. SC-RR-70-429, 1970 (unpublished).

[9]W. N. Asaad and E. H. S. Burhop, Proc. Phys. Soc. (London) 71, 369 (1958).

[10]E. J. McGuire, Phys. Rev. A 3, 587 (1971).

[11]J. G. Ferreira, M. O. Costa, M. I. Gonçalves, and L. Salgueiro, J. Phys. (Paris) 26, 5 (1965). The Coster-Kronig probabilities f_{13} reported by this group were derived under the assumption that $f_{23}=0$ and consequently are somewhat too high.

[12]R. Päschke, Z. Physik 176, 143 (1963).

[13]L. Persson and Z. Sujkowski, Arkiv Fysik 19, 309 (1961).

[14]P. Venugopala Rao, R. E. Wood, J. M. Palms, and R. W. Fink, Phys. Rev. 178, 1997 (1969).

[15]P. Venugopala Rao, J. M. Palms, and R. E. Wood, Phys. Rev. A 3, 1568 (1971).

[16]M. A. S. Ross, A. J. Cochran, J. Hughes, and N. Feather, Proc. Phys. Soc. (London) A68, 612 (1955).

[17]H. U. Freund and R. W. Fink, Phys. Rev. 178, 1952 (1969).

PHYSICAL REVIEW A VOLUME 4, NUMBER 6 DECEMBER 1971

Nonrelativistic Auger Rates, X-Ray Rates, and Fluorescence Yields for the $2p$ Shell*

D. L. Walters† and C. P. Bhalla
Department of Physics, Kansas State University, Manhattan, Kansas 66502
(Received 9 April 1971)

The Auger rates, x-ray rates, fluorescence yields, and $K\alpha$ linewidths are presented for all elements $Z=12$–55 and $Z=60$, 65, 70, 75, 80, and 85 when a vacancy is in the $2p$ shell. Numerical calculations have been performed using the Hartree-Fock-Slater approach with Herman, Van Dyke, and Ortenburger exchange. Comparisons of different exchange approximations on the Auger and x-ray total transition rates and the fluorescence yields are reported.

I. INTRODUCTION

There have been few extensive theoretical calculations involving the Auger process for the L shells. Rubenstein, [1] using a Hartree-Fock approach has calculated a number of transitions for $Z=18$, 36, and 47. Recently, McGuire[2] has performed extensive calculations using the Hartree-Fock-Slater (HFS) model for transitions to the L_1, L_2, and L_3 shells.

We have recently reported[3,4] that the technique used by McGuire[5,6] in calculating the Auger transitions for the K shell can lead to significant errors. The choice of exchange approximation can also have a pronounced effect on the Auger rates. The work of Herman, Van Dyke, and Ortenburger[7,8] (HVO) and others has shown that the inclusion of an inhomogeneity term in the free electron exchange approximation provides an improvement in the HFS model. The HVO approach is a straightforward technique yielding accurate orthonormal wave functions which can be easily adapted to Auger calculations.

The Auger transitions to the $L_1(2s)$ shell are strongly influenced by the L_1-$L_{2,3}X$ Coster-Kronig transitions. A comparison of the results of Talukdar and Chattarji, [9] McGuire, [2] and our own preliminary calculations involving the $2s$ shell indicates that care must be exercised in computing reliable Coster-Kronig transition rates. Difficulties arise in the accurate determination of the Coster-Kronig energies and in the validity of the nonrelativistic approach. Therefore, we do not intend to report on the $2s$ shell at this time. The L_2-L_3X Coster-Kronig transitions have also been neglected from the present work for similar reasons. Because of the L_2-L_3X transitions, calculations pertaining to the $2p$ shell more accurately refer to the L_3 shell at large atomic numbers.

The total Auger transition rates for a particular final-state configuration do not depend upon the coupling scheme (L-S, J-J, or intermediate coupling) used in calculating the rates. Therefore, the agreement between experiment and theory for Auger relative intensities should be best when viewed in terms of the final-state configurations. These Auger group rates may depend upon configuration interaction, however. A comparison of theory and experiment should reveal which elements are the most strongly influenced. Reliable theoretical Auger transition rates for the $2p$ shell have not been available to make such a comparison.

It is the purpose of this paper to present $2p$-shell Auger transition rates, x-ray transition rates, fluorescence yields, and $K\alpha$ x-ray linewidths for all elements from $Z=12$ to $Z=55$ and also for $Z=60$, 65, 70, 75, 80, and 85. We have employed the nonrelativistic HFS model with the HVO exchange